Structure and morphology of segmented polyurethanes: 4. Domain structures of different scales and the composition heterogeneity of the polymers

M. Xu*, W. J. MacKnight†, C. H. Y. Chen-Tsai and E. L. Thomas
Department of Polymer Science and Engineering, University of Massachusetts, Amherst, MA 01003, USA
(Received 14 May 1987; accepted 3 June 1987)

The morphology of polybutadiene containing polyurethanes has been studied by using small-angle light scattering (SALS), small-angle X-ray scattering (SAXS), phase contrast microscopy and electron microscopy. Domain structures having sizes of 1000, 100 and 10 nm are observed within these samples and are explained as the results of segregation on the molecular level, subchain level and segmental level, respectively. These phenomena are related to the molecular heterogeneity in chemical composition and average hard segment length. It has been found that because of the analogy in molecular structure with SBS block copolymers, segmented polyurethanes may form microdomains of soft and hard segments with more or less uniform size and regular arrangements in space.

(Keywords: segmented polyurethanes; compositional heterogeneity; segregation; morphology; scattering; microscopy)

INTRODUCTION

Segmented polyurethanes form multiphase polymers in the bulk. Because of the basic thermodynamic incompatibility of the segments, localized microphase separation occurs, leading to the well recognized domain structure, and the properties of the final bulk material are strongly influenced by the extent of microphase separation and the morphological characteristics of the domains. Numerous studies of the morphological features of the segmented polyurethanes have been carried out by means of microscopic and scattering techniques.

The small-angle X-ray scattering (SAXS) patterns of segmented polyurethanes usually show a distinct peak[1-7]. This is indicative of a quasi-periodic fluctuation in electron density within these materials. The periodicity given by the Bragg spacing corresponding to the scattering angle at peak intensity ranges from about 10 to 20 nm and it increases with increasing molecular weight of the soft segment[3,4]. Kimura *et al.*[4] have shown that, when the molecular weight of the soft segment is extrapolated to zero, the value of the spacing determined from SAXS measurements is consistent with the average length of the fully extended hard segments. These SAXS results are accepted as evidence for microphase separation of soft and hard segments and are used to characterize the domain structure of these materials in the size range of tens of nm.

Hard segment domains were observed as grains of 3–10 nm dimensions by Koutsky *et al.*[8] in solvent etched and iodine stained polyurethane samples by means of transmission electron microscopy. A fibrillar structure has been reported by Schneider *et al.* and the smallest fibrils observed were 20–30 nm in width[5]. Finer fibrils of 6 nm width have been observed by Fridman and Thomas[9].

Hard segment and soft segment domains can also organize to form crystalline superstructures, especially in the case of solution cast samples. Spherulites with diameters from several thousands of nm up to about 20 μm have been observed by small-angle light scattering (SALS), optical and electron microscopic methods[2,4,5,9-11]. Several models have been proposed to describe the structure of hard segment domains and their arrangement within the spherulite[2,5,9]. Hard segment rich amorphous 'globules' of several thousands of nm in diameter have been observed in the case of reaction injection moulded polyester/MDI/BDO polyurethanes[10]. They are preferentially present near the mould surface.

It has been found in the case of polybutadiene/2,4-TDI or 2,6-TDI based polyurethanes that because of the heterogeneity of the reaction system the macromolecules of the segmented copolymers can vary greatly in their chemical composition and average hard segment length, and will segregate during processing due to their poor compatibility or different solubility in solvents[12,13]. Compositional heterogeneity has also been detected recently for PCL/PET segmented polyesters[14] and PCL/MDI/BDO polyurethanes[15] by means of gel permeation chromatography (g.p.c.) and thin layer chromatography (t.l.c.). Thus, it is necessary to take into account both the microphase separation of hard and soft segments of the same chain into different domains, as is usually done, and also macrophase separation of macromolecules as a whole (segregation on the molecular level) in order to explain the morphology and properties of these materials. According to this idea the existence of

* Permanent address: Institute of Chemistry, Academia Sinica, Beijing, China
† To whom correspondence should be addressed

0032-3861/87/132183-07$03.00

Table 1 Overall compositions of the original polyurethanes

Samples	Molar composition PBD/TDI/BDO	Hard segment content (wt%)	Sol fraction content (wt%)
4T4	1/4.2/3	31.3	56
4T10	1/10.5/9	54.5	80

two hard segment T_g values, a unique transition behaviour of polybutadiene-containing polyurethanes can be explained from the compositional heterogeneity of the molecules[12].

Undoubtedly, the segregation of molecules as a whole will strongly influence the morphology of the samples. One of the important consequences to be expected is the existence of large-scale (much larger than the size of a molecule) domain structures. For crystallizable copolymers the situation is more complicated because of the difficulty in discriminating between the effects of crystallization and segregation of molecules with different compositions as the origin of the contrast between the domains and their surroundings. (The influence of molecular segregation on crystal morphology has been reported for a polyester–polyether segmented copolymer[16].) In this paper the domain structures of PBD/2,4-TDI/BDO based amorphous polyurethanes and their relations to segregation on different levels are studied.

EXPERIMENTAL

Materials

The same two PBD/2,4-TDI/BDO polyurethane samples, 4T4 and 4T10, described in the first paper of this series[12], were used. The details of the synthesis procedure have been described previously[17]. An anionically polymerized hydroxy terminated polybutadiene provided by Japanese Synthetic Rubber Company (JSR HTPBD) of $M_n = 2200$ was used as the soft segment. This macroglycol has an average hydroxy functionality of 1.97 and contains 55% vinyl butadiene, 35% *trans*-1,4, and 10% *cis*-1,4-butadiene units. Both samples have been separated into a sol fraction and a gel fraction by means of solvent extraction using dimethylformamide (DMF) as the solvent[12]. The overall compositions of the two original polyurethane samples are given in *Table 1*.

Small-angle light scattering

The photometric small-angle light scattering studies were performed using a one-dimensional position sensitive SALS detector with a Spectra-Physics He–Ne gas laser model 145 ($\lambda_0 = 632$ nm) as the light source[18,19]. The light scattered by the samples at different scattering angles in any azimuthal direction can be scanned by a Vidicon. The results were then digitized and stored by means of a multichannel analyser and can be input into the computer for further treatment. The scattering curves have been smoothed and the corrections to background and angular dependence of sensitivity have been considered. The photographic light scattering patterns were recorded on Polaroid type 52 film.

Small-angle X-ray scattering

The SAXS experiments were performed on the ORNSC 10 m SAXS camera. Details of the instrument have been given by Hendricks[20]. A 6 kW rotating anode X-ray generator (CuKα radiation), a graphic monochromator, pinhole collimators and a two-dimensional position-sensitive proportional counter were used. The source-to-specimen and specimen-to-detector distances were 1.62 and 5.15 m, respectively, which corresponds to an angular resolution of about 0.5 mrad.

Phase contrast optical microscopy

The sample films on glass slides were examined in a Zeiss Standard Junior microscope using tungsten light with an achromatic aplanatic phase contrast condenser (setting '2') with × 40/0.75 n.a. plane objective with × 10 eye piece. Photomicrographs were taken on Kodak Tri-X films using a standard 35 mm camera back-coupled to the Zeiss microscope.

Electron microscopy

A Jeol 100CX transmission electron microscope was operated at 100 kV at magnifications of 20 000–50 000 × using Kodak SO163 plates. Specimens were made by floating off the thin solution-cast films on glass slides in the water bath, and picking up on 300 mesh copper grids. Special precautions were taken to minimize electron beam damage of the samples and avoid radiation artefacts by focusing on an area and translating to an adjacent area for recording.

RESULTS

Small-angle light scattering

Films cast from DMF solutions of the two original samples, 4T4 and 4T10, and their gel fractions, 4T4G and 4T10G, were used for SALS studies. In all cases the scattering patterns are circularly symmetric with respect to the incident beam, and the intensity of the scattering by the gel samples is many times weaker than that of the original ones. The V_v scattering patterns of 4T4 and 4T4G samples, which have almost the same thickness, are given in *Figure 1*. Photometric measurements of the scattering were then performed in an arbitrarily selected azimuthal direction. The angular dependence of the V_v scattering is given in *Figures 2* and *3*. The scattering intensity decreases monotonically with increasing scattering angle for all samples. The scattering of a typical amorphous homopolymer, polymethylmethacrylate, has also been determined for comparison and is given in *Figure 3*.

The statistical treatment of light scattering from an isotropic medium exhibiting fluctuations in polarizability has been presented by Debye and Bueche[21]. They give the intensity of V_v scattering as follows:

$$I = K\langle\eta^2\rangle \int V(r) r^2 \sin hr/hr \, dr \qquad (1)$$

Here K is a proportionality constant, $\langle\eta^2\rangle$ is the mean square average polarizability, $V(r)$ is the correlation function for fluctuations in polarizability, and $h = (4\pi\sin\theta/2)/\lambda$, where λ is the light wavelength in the medium and θ is the scattering angle in the medium. Two types of correlation functions, the exponential function[2] and the Gaussian function[3] have been tested.

$$V(r) = \exp(-r/a_c) \qquad (2)$$

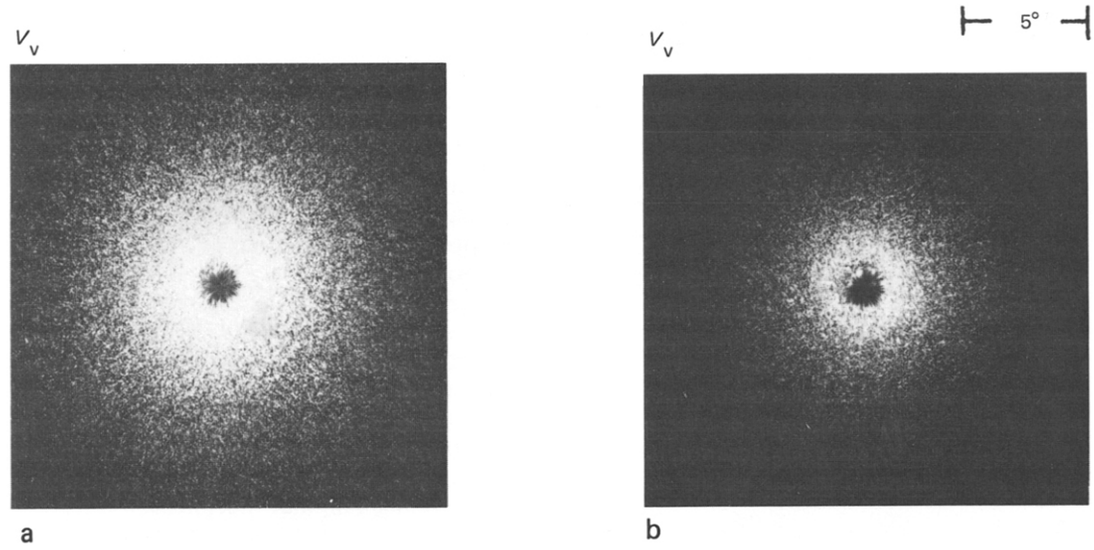

Figure 1 SALS V_v patterns of (a) 4T4 and (b) 4T4G

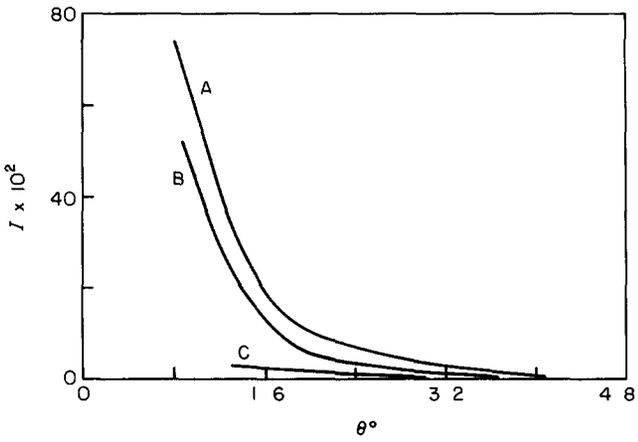

Figure 2 Angular dependence of V_v scattering: A, 4T4; B, 4T10; C, 4T4G

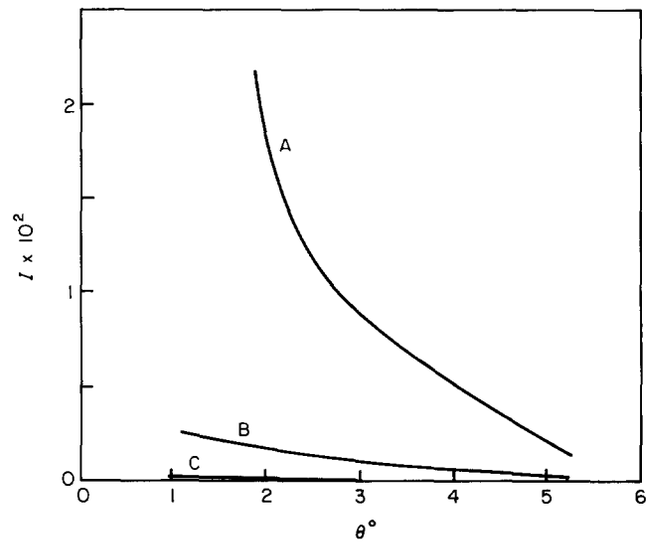

Figure 3 Angular dependence of V_v scattering: A, 4T4G; B, 4T10G; C, PMMA

$$V(r) = \exp(-(r/a_c)^2) \quad (3)$$

Parameter a_c represents the correlation distance of the fluctuation. It was found that equation (3) fits the experimental data better than equation (2). When the Gaussian function is used as the correlation function, equation (1) becomes

$$I = K\langle\eta^2\rangle a_c^3 \exp(-h^2 a_c^2/4) \quad (4)$$

Thus $\langle\eta^2\rangle$ and a_c can be determined from the slope and the intercept of a Guinier type plot, i.e. a plot of ln I *versus* h^2, which is given in *Figure 4* for samples 4T4, 4T4G, 4T10 and 4T10G. The a_c value for these samples is listed in *Table 2*. As the constant K was not calibrated for absolute Rayleigh ratio measurements, only the ratio of the mean square fluctuation for the original sample $\langle\eta^2\rangle$ to that of the relevant gel sample $\langle\eta^2\rangle_G$ is given in *Table 2*.

Small-angle X-ray scattering

The SAXS isointensity contour maps were found to be circularly symmetric for samples 4T4 and 4T10. The scattering intensity as a function of the scattering angle was then obtained from the contour map by a circular

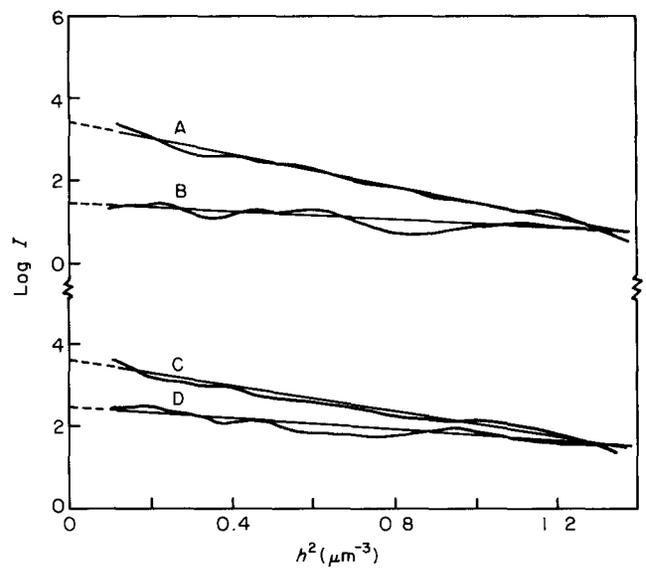

Figure 4 Logarithmic plot of SALS data: A, 4T4; B, 4T4G; C, 4T10; D, 4T10G

Table 2 SALS results

Sample	4T4	4T4G	4T10	4T10G
a_c (μm)	4.3	3.2	4.7	2.6
$\langle\eta^2\rangle/\langle\eta^2\rangle_G$	5.24		12.2	

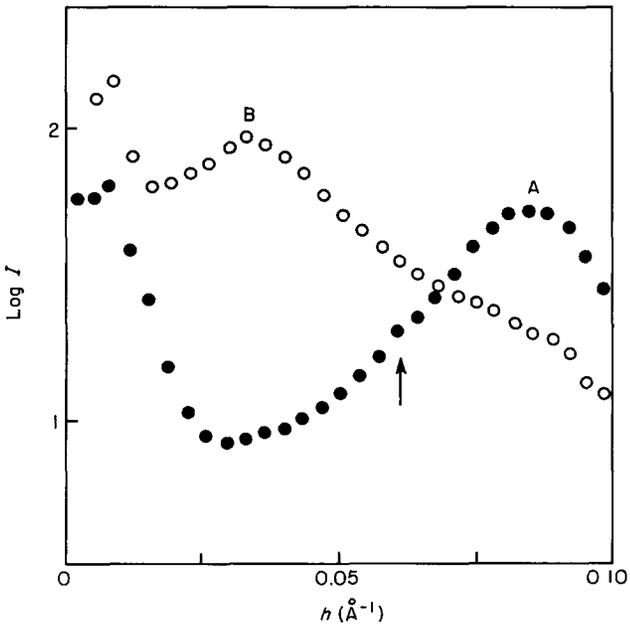

Figure 5 Circularly averaged SAXS data: A, 4T4; B, 4T10

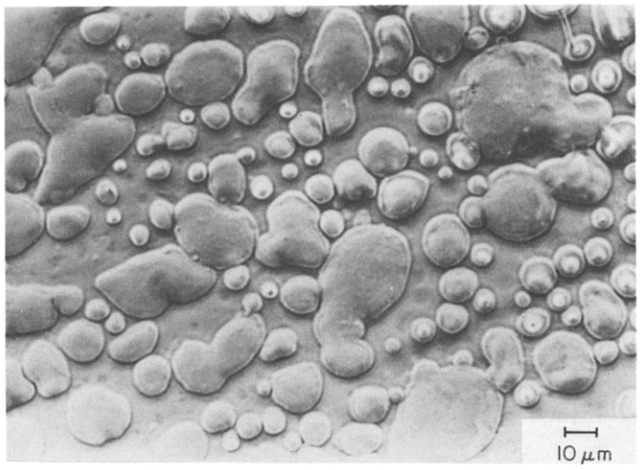

Figure 6 Thin film of samples 4T4 prepared by solvent (DMF) cast method; phase contrast condenser illumination by tungsten light

averaging procedure. The results for samples 4T4 and 4T10 are given in *Figure 5*. The scattering intensity exhibits maxima at scattering angles 1.188° and 0.462° for 4T4 and 4T10, respectively. Both peaks are very broad, and an obvious shoulder can be observed for 4T10 at about $\theta = 1.30°$.

Phase contrast optical microscopy

Figures 6 and *7* are phase contrast micrographs of samples 4T4 and 4T10 cast from their solutions in DMF. Domain structures can be observed in the size range from several thousand nm up to 50–70 μm. The domain structure has a higher volume fraction in films of sample 4T4 than in that of 4T10 and so is believed to be the result of segregation of soft-segment-rich macromolecules. For the gel samples 4T4G and 4T10G domains of μm size were observed only in a very few cases.

Electron microscopy

Substructures on the 10 to 100 nm level within the domain and matrix phases observed by phase contrast microscopy can be detected by means of the electron microscopy technique. *Figure 8* is an electron micrograph of the 4T4 sol fraction cast from its solution in DMF. It shows the heterogeneity of the macroscopic hard-segment-rich domains which are composed of spherical soft-segment-rich subdomains about 100 nm in diameter dispersed in a hard-segment-rich matrix. Sometimes a group of these grains may form regions of 1 to 2 μm having detectable contrast with respect to their surroundings. Similar morphological features have been observed for solution-cast films of 4T10 sol fraction. Electron microscopic studies show that for gel fractions, hard-segment-rich domains of more than μm size were seldom observed, which is consistent with the results of phase contrast microscopy. Substructures can be detected in some cases in the soft-segment-rich regions. *Figure 9* is

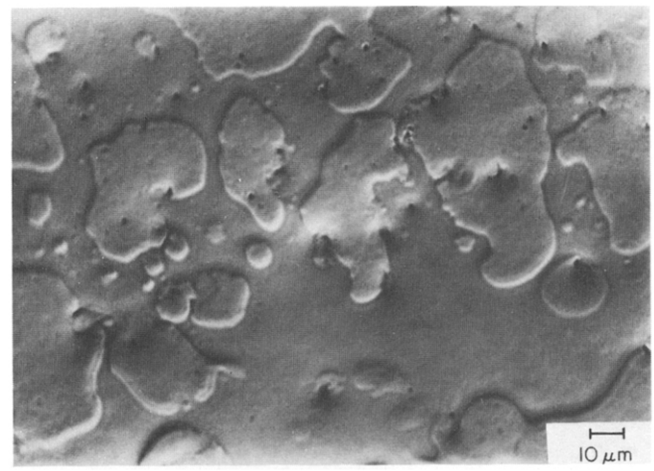

Figure 7 Thin film of sample 4T10 prepared by solvent (DMF cast method; phase contrast condenser illumination by tungsten light)

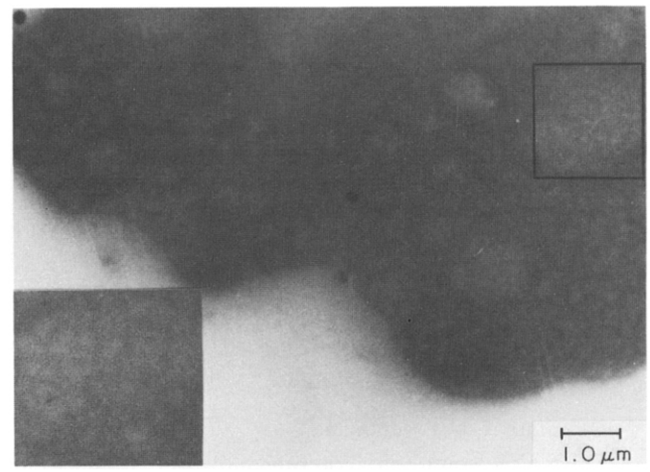

Figure 8 Electron micrograph of a DMF solution cast thin film from 4T4S sample. A higher magnification of the squared area is shown in the left-hand side lower corner

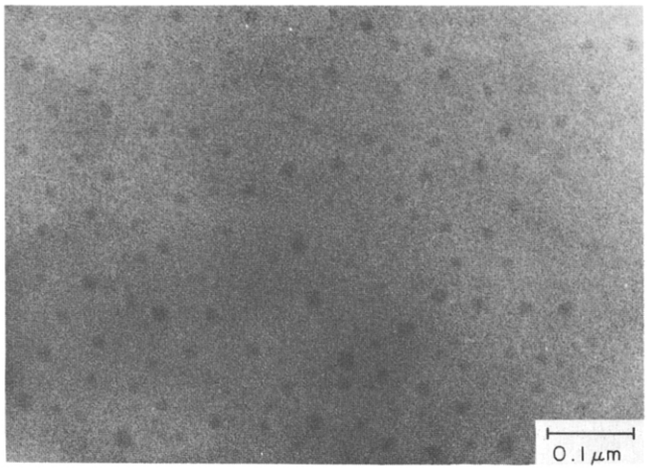

Figure 9 Electron micrograph of an MIBK solution cast thin film from 4T4G sample

Table 3 Characterization of polyurethanes

Sample	Percentage of fractions (wt%)	Hard segment content (wt%)	Composition TDI/PBD (mol)
4T4		31.3	4
4T4-1	62	17.0	2
4T4-2	38	53.0	9.3
4T10		54.5	10
4T10-1	20	10.5	1.3
4T10-2	80	67.5	17

an example for 4T4 gel fraction cast from solution in methyl isobutyl ketone (MIBK). Small dark spots of about 20–40 nm in diameter are found to be arranged irregularly from 10 to 100 nm apart in a bright matrix. These spots could be microdomains containing relatively more hard segments than their surroundings.

DISCUSSION

The results of the SALS experiments indicate the existence of domain structures corresponding to the fluctuation in polarizability with correlation distance of the order of 10^3 nm within these polyurethane samples, and micrographs also show the presence of these large domains. In this case, both hard and soft segments of the copolymers are amorphous, so the large-scale supermolecular structure cannot be the result of crystallization, but can only be related to some kind of compositional heterogeneity within the samples. It is, of course, quite impossible to form the large heterogeneities observed if the molecules making up the polymer are all more or less uniform, with small fluctuations in composition and hard segment sequence length around the stoichiometric values expected from the polymerization conditions. It has already been shown in the first paper of this series[12] that in the case of polybutadiene-containing polyurethanes the macromolecules are quite heterogeneous both with respect to the composition and average hard segment length, and this is due to the poor compatibility of the reaction components. Thus, they can be approximately considered to be blends of two segmented copolymers, a relatively soft-segment-rich fraction (fraction 1) and a relatively hard-segment-rich fraction (fraction 2). The heterogeneity of samples 4T4 and 4T10 determined in ref. 12 is listed in *Table 3*. Because of the poor uniformity of the solution-cast films it is very difficult to obtain the precise domain content from the micrographs. However, the results of crude estimates compare reasonably well with the fractions 1 and 2 contents given in *Table 3*. It is thus clear that the large domain structures are the result of molecular level segregation within these polyurethane samples, i.e. they are blends of segmented copolymers.

It has been supposed[12] that the gel fractions are rather homogeneous and mainly composed of the soft-segment-rich molecules, as only the lower hard-segment glass transition is observed from differential scanning calorimetry (d.s.c.). However, the d.s.c. technique is not very sensitive to composition. The microscopic observations of this study indicate the existence of a very few hard-segment-rich domains within the gel fractions, and their light scattering intensity is also much larger than that of PMMA, which only has heterogeneities on scales much less than the wavelength of the radiation (6328 nm). We assume that the light scattering of these samples is mainly due to compositional heterogeneity and can be described by an ideal two-phase model. The original sample and its gel fraction are both composed of the two phases corresponding to the same fraction 1 and fraction 2 pair and are only different in content. For an ideal two-phase model we have[22]:

$$\langle \eta^2 \rangle = (\alpha_1 - \alpha_2)^2 \phi_1 \phi_2 \tag{5}$$

and

$$\phi_1 + \phi_2 = 1 \tag{6}$$

Here α_i and ϕ_i are the polarizability and volume fraction of the ith phase respectively. Because $\alpha_1 - \alpha_2$ has the same value for the original sample and its gel fraction as has been assumed, one can estimate the phase content of the gel fraction from that of the original sample and the ratio $\langle \eta^2 \rangle / \langle \eta^2_G \rangle$. The results are given in *Table 4*, and this confirms that the gel fractions are really quite homogeneous, and their hard-segment-rich fraction is less than 5% by volume.

Information about the segmental level segregation was obtained from SAXS data. The existence of an intensity maximum indicates not only that the hard and soft segments are segregated within these polyurethanes, but even that their domains may be arranged more or less regularly in space since they exhibit a periodicity in changing electron density. A similar phenomen has been reported by Lagasse[6] for a 2,4-TDI/PBD based polyurethane with a mixture of 2-ethyl-1,3-hexanediol and *N*,*N*-bis(2-hydroxypropyl)aniline as the chain extender. An intensity maximum in SAXS is usually observed for crystalline polymers and is referred to as the long period. For amorphous polymers the SAXS curves

Table 4 Volume fractions of the two phases in original samples and their gel fractions

Sample	ϕ_1 (%)	ϕ_2 (%)
4T4	63.4	36.6
4T4G	95.4	4.6
4T10	21.6	78.4
4T10G	98.6.	1.4

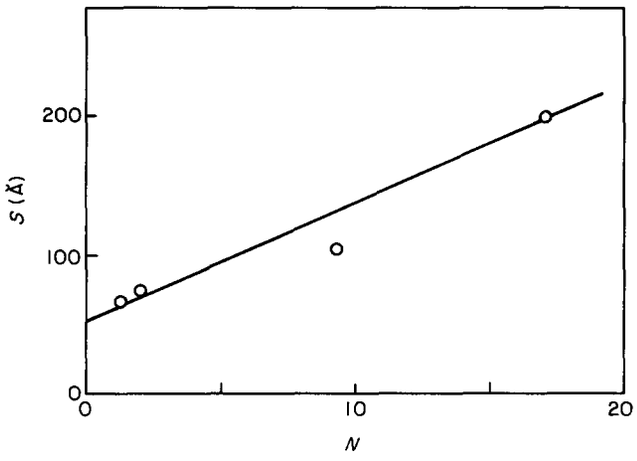

Figure 10 Dependence of the spacings from SAXS measurements on the mole ratio of TDI/PBD

show maxima only in cases such as AB and ABA diblock and triblock copolymers[23-25] because of the uniform size and regular lattice-like arrangements of the domains in these polymers resulting from their highly regular molecular structure. Thus, these SAXS results may imply that the segmented polyurethane, a multiblock copolymer, can also form regular domain structures like the well known ABA triblock copolymers.

As has been mentioned before, in addition to the main peak there is a small-intensity peak located at larger scattering angles for the 4T10 sample. A very weak maximum, although it is not very clear due to superposition, can also be found for 4T4 at smaller angles, as indicated in *Figure 5* by an arrow. As domains of fraction 1 and fraction 2 are formed in these samples as a result of macroscopic phase separation, so the two SAXS peaks should be evidence for hard and soft segment segregations and microdomain arrangements in both hard-segment-rich and soft-segment-rich regions.

Figure 10 is a plot of the spacing *versus* the number of TDI units in the hard segments. A linear dependence is obtained. The intercept on the ordinate is 5.2 nm, which is very close to the value of 4.8 nm for polybutadiene molecules with molecular weight 2200 in θ-conditions[26]. Subtraction of the size of the soft segment microphase (5.2 nm) from the SAXS spacings will give the thickness of the hard segment regions. It is found that for soft-segment-rich domains (fraction 1) the thickness of the hard segment regions is almost equal to their extended lengths but the thickness of hard segment regions in hard-segment-rich domains (fraction 2) is two to three times less than the extended length of the hard segment. This implies that short hard segments (TDI/PBD mole ratio equal to about 2) almost have the extended chain conformation, but longer hard segments are coiled.

The internal structure of the hard and soft segment microdomain were not detected directly in the electron microscopy studies because they are too small and thus below the resolution limit. The substructures within the hard-segment-rich and soft-segment-rich regions observed by electron microscopy could be structures of another scale level, intermediate between the microdomains of segments and domains of macromolecules as a whole.

We assume that these substructures are the results of segregation of molecular subchains of different compositions and average hard segment lengths. The original polyurethane samples contain different kinds of segmented macromolecules with very different compositions and average hard segment lengths. In the solution casting process, macrophase separation takes place, resulting in a phase with long average hard segment lengths and one with very short average hard segment lengths. After that, because of very poor compatibility or differences in solubility, microphase separation is still possible, provided that there is enough chain mobility, and this results in the substructures observed by electron microscopy. Microdomains of hard and soft segments are assumed to exist in these microphases as well as in the macrophases.

Under the conditions of synthesis, it is not reasonable to expect two populations containing monodisperse hard segment lengths. Rather, a distribution of hard segment lengths must exist in both macrophases.

CONCLUSIONS

Polybutadiene containing polyurethanes synthesized in bulk have been shown to contain two fractions of segmented macromolecules with quite different composition and average hard segment length.

The morphological complexity of these segmented polyurethanes can be interpreted by taking into account the domain formation due to the segregation phenomena on different levels, namely, macrophase separation and microphase separation. As nonuniformity of the molecules with respect to chemical composition and average hard segment length is a common phenomenon for segmented copolymers, it is postulated that the general morphological features observed in polybutadiene containing polyurethanes should also be very useful for understanding the morphology–property relationships of other segmented copolymers.

ACKNOWLEDGEMENTS

We are grateful to the Army Research Office, Durham, under Grant No. DAAG 29 80 C0054, and the National Science Foundation, Grant CPE-8118232, Chemical and Process Engineering Program, for partial support of this research.

REFERENCES

1 Bonart, R. *J. Macromol. Sci.* (*B*) 1968, **2**, 115
2 Samuels, S. L. and Wilkes, G. L. *J. Polym. Sci.* (*C*) 1973, **43**, 149
3 Wilkes, C. E. and Yusek, C. S. *J. Macromol. Sci.* (*B*) 1973, **7**, 157
4 Kimura, I., Ishihara, H., Ono, d H., Yoshihara, N., Nomura, S. and Kawai, H. *Macromolecules* 1974, **7**, 355
5 Schneider, N. S., Desper, C. R., Illinger, J. L., King, A. O. and Barr, D. *J. Macromol. Sci.* (*B*) 1975, **11**, 527
6 Lagasse, R. R. *J. Appl. Polym. Sci.* 1977, **21**, 2489
7 Van Bogart, J. W. C., Gibson, P. E. and Cooper, S. L. *J. Polym. Sci., Polym. Phys. Edn.* 1983, **21**, 65
8 Koutsky, J. A., Hien, N. V. and Cooper, S. L. *J. Polym. Sci., Polym. Lett. Edn.* 1970, **8**, 353
9 Fridman, I. D. and Thomas, E. L. *Polymer* 1980, **21**, 388
10 Fridman, I. D., Thomas, E. L., Lee, L. J. and Macosko, C. W. *Polymer* 1980, **21**, 393
11 Chang, A. L. and Thomas, E. L. *Am. Chem. Soc., Adv. Chem. Ser.* 1979, **176**, 31
12 Xu, M., MacKnight, W. J., Chen, C. H. Y. and Thomas, E. L. *Polymer* 1983, **24**, 1327

13 Chen, C. H. Y., Briber, R. M., Thomas, E. L., Xu, M. and MacKnight, W. J. *Polymer* 1983, **24**, 1333
14 Xu, M., Ye, M. L., Shi, L. H., Zhu, C., Ma, D. Z. and Luo, X. L. *Polym. Commun. (China), Eng. Edn.* 1985, No. 1, 63
15 Xu, M., Li, P. J., Wang, Y., Luo, X. L., Liu, Y. and Ma, D. Z. *Polym. Commun. (China), Eng. Edn.* to be published
16 Xu, M., Hu, S. R., Wu, M. Y., Chen, C. F. and Jin, Y. Z. *Polym. Commun. (China)* 1982, No. 1, 27
17 Brunette, C. M., Hsu, S. L., Rossman, M., MacKnight, W. J. and Schneider, N. S. *Polym. Eng. Sci.* 1981, **21**, 668
18 Wasiak, A., Peiffer, D. and Stein, R. S. *J. Polym. Sci., Polym. Lett. Edn.* 1976, **14**, 381
19 Russell, T. P., Koberstein, J., Prud'homme, R., Misra, A. and Stein, R. S. *J. Polym. Sci., Polym. Phys. Edn.* 1978, **16**, 1879
20 Hendricks, R. W. *J. Appl. Crystallogr.* 1978, **11**, 15
21 Debye, P. and Bueche, A. M. *J. Appl. Phys.* 1949, **20**, 518
22 Stein, R. S. in 'Optical Behavior of Polymer Blends', 'Polymer Blends', Vol. 1, (Eds. D. R. Paul and S. Newman), Academic Press, New York, 1978, Ch. 9
23 Hashimoto, T., Fujimara, M. and Kawai, H. *Macromolecules* 1980, **13**, 1660
24 Roe, R. J., Fishkis, M. and Chang, J. C. *Macromolecules* 1981, **14**, 1091
25 Richards, R. W. and Thomason, J. L. *Polymer* 1981, **22**, 581
26 Brandrup, J. and Immergut, E. H. 'Polymer Handbook', Interscience Publishers, 1967